



The Modal Analysis of a Motorcycle in Straight Running and on a Curve

V. COSSALTER*, R. LOT and F. MAGGIO

Department of Mechanical Engineering, University of Padova, Via Venezia 1; 35131 Padova, Italy

(Received: 5 September 2002; accepted in revised form: 8 November 2002)

Abstract. The vibrational modes (generalized) of a two-wheel vehicle are studied in several trim configurations. The modal analysis is carried out on a 3D non-linear mathematical model, developed using the natural coordinates approach. A special procedure for evaluating the steady state solutions in straight running and on a curve is proposed. The paper presents detailed results of the modal analysis for a production sports motorcycle. Furthermore, the influence of speed and lateral (centripetal) acceleration on stability, shape and modal interactions (coupling) is highlighted. Finally, consistency between the first experimental tests and simulation results is shown.

Key words: Motorcycle stability, Weave, Wobble, Capsize.

1. Introduction

The modal and stability analysis of the motorcycle gives important information about riding safety, handling capabilities and riding comfort. This is the main reason for much research effort over the last 30 years to determine the free-modes of a motorcycle. Sharp presented a pioneering work [1] in 1971, where he analyzed the modes in straight running and their implications on control. This motorcycle model was quite simple, but the information that it supplied is still fundamental. The straight-running vibrational modes were analyzed in many subsequent works adding information about the effects of frame compliance [2–6], fork flexibility [7] and tire properties [8, 9]. The topic was also studied by means of the energy flow method [10]. In spite of this, the literature offers us very few articles on the modal analysis on a curve due to the fact that the dynamics in a leaning configuration can only be described with complex equations. The main difficulty lies above all in developing a tire modeling which correctly describes the behavior at large camber angles. At first, the cornering modes were studied by Koenen and Pacejika [11] in 1980 and the influence of several parameters was discussed later by the same authors [12]. Other works are very recent [8, 13] and focus on stability changes (with respect to the straight-running case) and on the coupling phenomena. A more complete state of the art can be found in [14].

The free-modes of the motorcycle can be grouped as *in-plane* modes and *out-of-plane* modes. The modes of the first family, which involve the motion of the motorcycle in its symmetrical plane, are the pitch, bounce, front and rear wheel hops. The modes of the second group, which involve the lateral motion of the vehicle, are the capsize, weave, wobble and rear wobble modes. The *in-plane* modes only affect the riding comfort, whereas the *out-of-plane* modes strongly affect the stability and safety of the motorcycle. In straight running, *in-plane*

* Author for correspondence: Tel.: +39-049-8276793, Fax: +39-049-8276785, e-mail: vito@mecc.unipd.it

and *out-of-plane* modes are uncoupled and can be examined separately [1]. The coupling occurs in cornering motion [8, 11, 13] because of the camber angle, which modifies the mode shapes, their damping ratios and their frequencies.

This paper presents a numerical modal analysis of a sports motorcycle, both in straight running and on a curve. Section 2 provides a brief description of the mathematical motorcycle model, which has eleven degrees of freedom. It is not linear and it was developed with the ‘natural coordinates’ method [16, 17]. A complete description of the model can be found in reference [15]. Some experiments were carried out in order to verify the reliability of this model, finding a good degree of consistency between simulations and experimental data [19, 15]. Section 3 explains the procedure to determine the vibration modes, which basically consists of three steps: first the steady state condition of the motorcycle is found, then the equations of motion are linearized and finally the eigenvalue problem is solved. Section 4 presents a detailed analysis of eigenvalues and eigenvectors of a sports motorcycle, whose geometrical and inertial characteristics have already been measured [15]. The influence of speed on the straight running modes was studied, varying it from 5 up to 70 m/s. Simulations were repeated on a curve, considering lateral acceleration up to 7.5 m/s^2 . A physical interpretation of the phenomena is given.

Section 5 compares the simulations with the first experimental tests, showing a good degree of consistency between them.

2. Motorcycle and Tire Model

The multi-body model of the motorcycle consists of a system of six bodies. The main one is the rear assembly, which includes the chassis, the engine and the tank. The rider is considered a rigid body attached to the rear assembly. The second body is the front assembly, which is comprised of the handlebars, the steering plates and the fork sprung parts. The swinging arm and the rear braking device form the body called ‘rear unsprung mass’ whereas the ‘front unsprung mass’ includes the unsprung part of the forks and the front braking devices. The last two bodies are the wheels. The model has eleven degrees of freedom, as shown in Figure 1. Three coordinates and three angles (roll, pitch and yaw) are used to locate the rear assembly and to define its spatial orientation. A further five degrees of freedom describes the relative motion between the motorcycle parts, such as the steering angle, the suspension travels and the spinning rotations of both wheels. The front suspension is telescopic, whereas the rear one is a swinging arm type. The transmission of the engine power to the rear wheel is obtained through a chain drive. The model takes into account the aerodynamic effects such as drag, lift and lateral forces. The input quantities of the model are the same as a real motorcycle, that is, the steering torque, the braking torque and the propulsion torque, except for the lean rider motion which is not taken into account.

In this model, the bodies are considered perfectly rigid because sports motorcycles have very stiff frames and the structural flexibility has a marginal effect on stability [4]. Moreover, the comparison between the structural and in-motion modes shows only a low interaction between them [5].

The tire model [28] is one of the most important features of this motorcycle model. It accurately describes the geometry of the tread, which is fundamental in evaluating tire behavior at large camber angles, and the elasticity of the carcass (see Figure 2). The external contact forces are calculated as a function of the slip velocity and camber angle using the Pacejika formulas [21]. The corresponding internal elastic reactions are calculated as a function of the

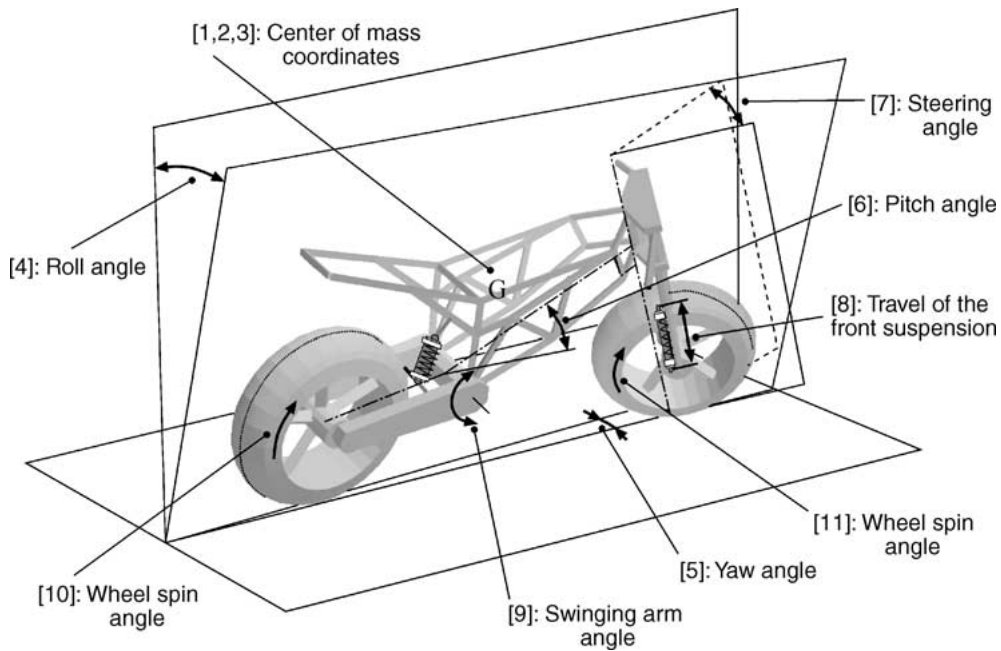


Figure 1. Eleven degrees of freedom motorcycle model.

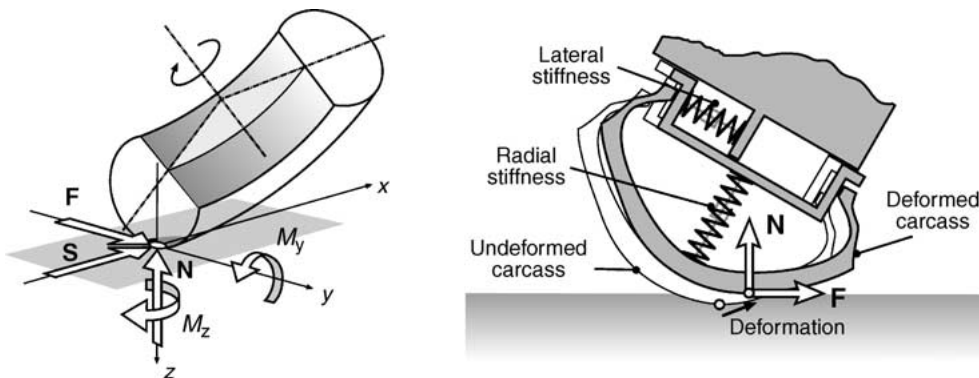


Figure 2. Elastic tire model.

tire deformations and camber angle. The model also calculates the position of the contact point, as function of the camber angle and tire deformations. All tire forces are applied on this point, which corresponds to the center of the contact patch. Tire torques consist of the rolling resistance torque M_y and the yaw torque M_z , whereas the overturning moment is not included. In fact, the latter were due to the assumption of a conventional contact point, as shown in the references [21–23]. This model properly describes the behavior of the tire both in steady state and in transient conditions, as shown in references [15, 28].

3. Procedure of Modal Analysis

The procedure consists of three steps: the calculation of the steady state condition, the linearization of the equations of motion and the solution of the eigenvalue problem. The particularities

of the proposed procedure, which are described in the next sections, are the following:

1. the equations of motion were written in a moving reference frame;
2. the steady state condition were calculated by solving a set of algebraic equations;
3. the eigenvalue problem was formulated in dependent coordinates and then converted to a standard form.

The motorcycle model and the modal analysis procedure were implemented in a Fortran program¹, which makes it possible to perform a complete dynamic analysis of a motorcycle.

3.1. THE MOVING FRAME APPROACH FOR THE EQUATIONS OF MOTION

A brief description of the equations of motion, which are described completely in reference [15], is given here. A dependent coordinates formulation [16, 17] is used. Each body is identified by means of a transformation matrix, which contains the three coordinates of a basic point and the nine components of its unit vectors. Thus, each body is described by means of 12 dependent coordinates. Since some of them are shared between two or more bodies, the entire system is described using $n = 45$ coordinates, which are collected in the vector \mathbf{q} . The motorcycle has only $f = 11$ degrees of freedom and so it is necessary to formulate a set of $m = n - f = 34$ independent constraint equations, as follows:

$$\Phi(\mathbf{q}) = 0 \quad (1)$$

The application of the Lagrange's approach to the constrained system yields to a set of $n = 45$ implicit equations of motion:

$$\mathbf{F}(\mathbf{q}, \dot{\mathbf{q}}, \ddot{\mathbf{q}}, \boldsymbol{\lambda}, \mathbf{u}) = 0 \quad (2)$$

where $\boldsymbol{\lambda}$ are the Lagrange's multipliers and $\mathbf{u} = \{\tau, M_P, M_{Bf}, M_{Br}\}^T$ is the control inputs vector, which consist of the steering torque τ , propulsive torque M_P and front and rear braking torques M_{Bf} and M_{Br} . The proper description of the tire deformability requires the six additional coordinates (collected in the vector \mathbf{q}'), which are the lateral, radial and torsional deformations of both tires. Thus, $n' = 6$ additional equations, which describe the tire behavior, are introduced:

$$\mathbf{P}'(\mathbf{q}, \dot{\mathbf{q}}, \mathbf{q}', \dot{\mathbf{q}}') = 0 \quad (3)$$

The steady state turning can be defined using just two independent parameters, which are the speed V and the curvature C of the circular path followed by the rear contact point. Even if this motion is easily recognized as a steady state condition, the coordinates \mathbf{q}, \mathbf{q}' in equations (1)–(3) still depend on time. This problem can be avoided by re-writing the equations with respect to an opportune moving reference frame \mathbf{R}_m , defined by means of the following 4×4

¹Named *FastBike*, in use at the Department of Mechanical Engineering only.

transformation matrix [18]:

$$\begin{aligned} \mathbf{T}_f^m &= \mathbf{T}_R\left(0, 0, \frac{1}{C}\right) \mathbf{R}_Z(\psi) \mathbf{T}_R\left(0, 0, -\frac{1}{C}\right) \\ &= \begin{bmatrix} \cos(\psi) & -\sin(\psi) & 0 & \frac{\sin(\psi)}{C} \\ \sin(\psi) & \cos(\psi) & 0 & \frac{1-\cos(\psi)}{C} \\ 0 & 0 & 1 & 0 \\ 0 & 0 & 0 & 1 \end{bmatrix} \end{aligned} \quad (4)$$

where \mathbf{R}_Z is the rotational operator upon the Z axis and \mathbf{T}_R is the translational one, as shown in Figure 3. Moreover, the yaw angle corresponds to $\psi = VCt$.

The coordinates of a generic point $\mathbf{P} = \{x, y, z, 1\}^T$ or a vector $\mathbf{v} = \{u, v, w, 0\}^T$, initially known with respect to the fixed reference frame \mathbf{R}_f , can be re-written in the moving frame \mathbf{R}_m using the transformation \mathbf{T}_f^m as follows:

$$\mathbf{P}_m = \mathbf{T}_f^m \mathbf{P}_f \quad \mathbf{v}_m = \mathbf{T}_f^m \mathbf{v}_f \quad (5)$$

For the whole system, the relationship between the fixed frame coordinates \mathbf{q} and the moving frame coordinates \mathbf{p} is obtained by assembling the overall transformation matrix \mathbf{T}_C , as follows:

$$\begin{Bmatrix} \mathbf{q} \\ 1 \end{Bmatrix} = \mathbf{T}_C(\psi) \begin{Bmatrix} \mathbf{p} \\ 1 \end{Bmatrix} \quad (6)$$

where \mathbf{T}_C is a square matrix of size $n + 1 = 46$. The coordinates \mathbf{q}' do not require any transformation because they were already defined with respect to a moving frame.

By substituting expression (6) into equations of motion (2), one obtains the equations with respect to the moving frame \mathbf{R}_m , which depend on the speed V and on the curvature C , but do not depend on the yaw angle ψ :

$$\mathbf{F}_m(\mathbf{p}, \dot{\mathbf{p}}, \ddot{\mathbf{p}}, \boldsymbol{\lambda}, \mathbf{u}; C, V) = 0 \quad (7)$$

The same substitution was done for the constraint equations (1), which did not alter their initial form:

$$\Phi(\mathbf{p}) = 0 \quad (8)$$

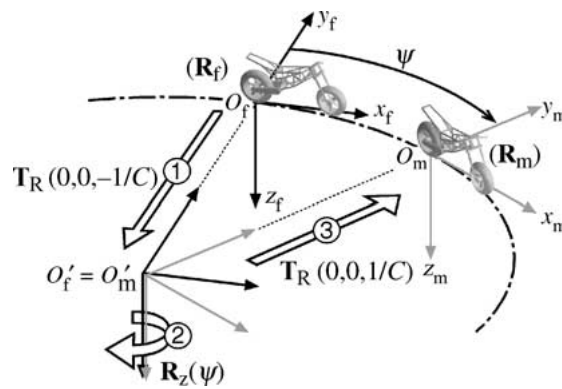


Figure 3. Fixed and moving frame.

This substitution was also applied to the tire equations (3), obtaining:

$$\mathbf{P}'_m(\mathbf{p}, \dot{\mathbf{p}}, \mathbf{q}', \dot{\mathbf{q}}'; C, V) = 0 \quad (9)$$

The result is a set of $n + m + n' = 85$ 2nd order differential-algebraic equations:

$$\mathbf{H}_m(\mathbf{p}, \dot{\mathbf{p}}, \ddot{\mathbf{p}}, \mathbf{q}', \dot{\mathbf{q}}', \boldsymbol{\lambda}, \mathbf{u}) = \begin{Bmatrix} \mathbf{F}_m \\ \boldsymbol{\Phi} \\ \mathbf{P}'_m \end{Bmatrix} \quad (10)$$

where the input vector quantities \mathbf{u} are assigned and the others are unknown.

3.2. THE STEADY STATE CONDITION

In multibody analysis, the steady state configuration of a system is usually found by integrating the equations of motion until the desired state is reached. This approach has at least two critical aspects: a control system is needed and the dynamic simulations are time consuming. These disadvantages are remarkable in motorcycle modeling, because the vehicle is intrinsically unstable and it is not easy to design a control, which was simultaneously quick, stable and steady state error free.

In this paper a different approach is followed and the steady state condition is found by solving the corresponding inverse dynamic problem. In fact, the steady state equations can be derived from the dynamic equations (10) by simply imposing a constant value to the variables $\mathbf{p} = \mathbf{p}_0$, $\mathbf{q}' = \mathbf{q}'_0$, $\boldsymbol{\lambda} = \boldsymbol{\lambda}_0$ and by setting to zero their derivative $\dot{\mathbf{p}} = \ddot{\mathbf{p}} = 0$ and $\dot{\mathbf{q}}' = 0$. In the input vector \mathbf{u} , the braking torques are both null whereas the steering torque τ_0 and the propulsive torque M_{p0} are unknown. Thus, for any given values of speed V and curvature C , the following set of pure algebraic equations is obtained:

$$\mathbf{H}_{m,0}(\mathbf{p}_0, \mathbf{q}'_0, \boldsymbol{\lambda}_0, \tau_0, M_{p0}; C, V) = 0 \quad (11)$$

In these equations, there are two redundant unknowns with respect to the number of equations, which leave two degrees of freedom to the system. This indeterminacy has to be resolved by adding two further constraint equations, such as by fixing the rear contact point \mathbf{P}_r on the origin of the moving frame \mathbf{R}_m :

$$\begin{aligned} x_{Pr}(\mathbf{p}_0, \mathbf{q}'_0) &= 0 \\ y_{Pr}(\mathbf{p}_0, \mathbf{q}'_0) &= 0 \end{aligned} \quad (12)$$

The final set of equations can be numerically solved for each value of curvature C and speed V , finding the steady state solution. In particular, the straight running motion can be studied by simply putting $C = 0$ into equations (11) and (12).

3.3. MODAL ANALYSIS IN DEPENDENT COORDINATES

Starting from the steady state solution, the equations of motion can be linearized and the perturbation analysis can be performed. In the dependent coordinates formulation, the linearized equations had to be rearranged before solving the eigenvalue problem, otherwise some modes without physical meaning were found [16, 17].

In the neighborhood of a known solution the variables can be written as:

$$\{\mathbf{p}, \mathbf{q}', \boldsymbol{\lambda}\}^T = \{\mathbf{p}_0, \mathbf{q}'_0, \boldsymbol{\lambda}_0\}^T + \{\Delta\mathbf{p}, \Delta\mathbf{q}', \Delta\boldsymbol{\lambda}\}^T \quad (13)$$

where $\{\Delta \mathbf{p}, \Delta \mathbf{q}', \Delta \boldsymbol{\lambda}\}^T$ is the vector of the infinitesimal variations. By linearizing the equations of motion (2) and the constraint equations (1) with starting point $\{\mathbf{p}_0, \mathbf{q}'_0, \boldsymbol{\lambda}_0\}^T$, the following equations are obtained:

$$\mathbf{M}\Delta\ddot{\mathbf{p}} + \mathbf{C}\Delta\dot{\mathbf{p}} + \mathbf{K}\Delta\mathbf{p} + \mathbf{K}_\phi\Delta\mathbf{p} + \boldsymbol{\Phi}_p^T\Delta\boldsymbol{\lambda} = 0 \quad (14)$$

$$\boldsymbol{\Phi}_p\Delta\mathbf{p} = 0 \quad (15)$$

where \mathbf{M} , \mathbf{C} and \mathbf{K} are respectively the mass, damping and stiffness matrices of the system. Moreover, $\boldsymbol{\Phi}_p$ is the Jacobian matrix of the constraint equations and \mathbf{K}_ϕ is the stiffness contribution to constraints, defined by:

$$\mathbf{K}_\phi = \sum_{k=1}^{m-n} \lambda_{0k} \mathbf{H}_k \quad (16)$$

where \mathbf{H}_k is the Hessian of k th constraint equation.

The dependent coordinates formulation can be transformed into an independent coordinates formulation using the coordinates transformation:

$$\Delta\mathbf{p} = \mathbf{R}\mathbf{z} \quad (17)$$

where \mathbf{R} is the projection matrix and \mathbf{z} is a vector of independent coordinates [16, 17]. The projection matrix \mathbf{R} can be found from the singular value decomposition (SVD) of the constraint jacobian matrix:

$$\boldsymbol{\Phi}_p\mathbf{R} = 0 \quad (18)$$

Thus, equation (15) disappears and by substituting expression (17) into equation (14) and by pre-multiplying them for \mathbf{R}^T , the equations becomes:

$$\mathbf{R}^T\mathbf{M}\mathbf{R}\ddot{\mathbf{z}} + \mathbf{R}^T\mathbf{C}\mathbf{R}\dot{\mathbf{z}} + \mathbf{R}^T\mathbf{K}\mathbf{R}\mathbf{z} + \mathbf{R}^T\mathbf{K}_\phi\mathbf{R}\mathbf{z} + (\boldsymbol{\Phi}_p\mathbf{R})^T\Delta\boldsymbol{\lambda} = 0 \quad (19)$$

or, in a more compact form:

$$\tilde{\mathbf{M}}\ddot{\mathbf{z}} + \tilde{\mathbf{C}}\dot{\mathbf{z}} + \tilde{\mathbf{K}}\mathbf{z} = 0 \quad (20)$$

where:

$$\begin{aligned} \tilde{\mathbf{M}} &= \mathbf{R}^T\mathbf{M}\mathbf{R} \\ \tilde{\mathbf{C}} &= \mathbf{R}^T\mathbf{C}\mathbf{R} \\ \tilde{\mathbf{K}} &= \mathbf{R}^T(\mathbf{K} + \mathbf{K}_\phi)\mathbf{R} \end{aligned} \quad (21)$$

and the last term disappears. From this point, the modal analysis is carried out in the standard way.

4. Results

4.1. EIGENVALUES

The following plots show the results of many simulations. Each graph represents the complex eigenvalues calculated for a fixed lateral acceleration and several speeds from 5 to 70 m/s (with

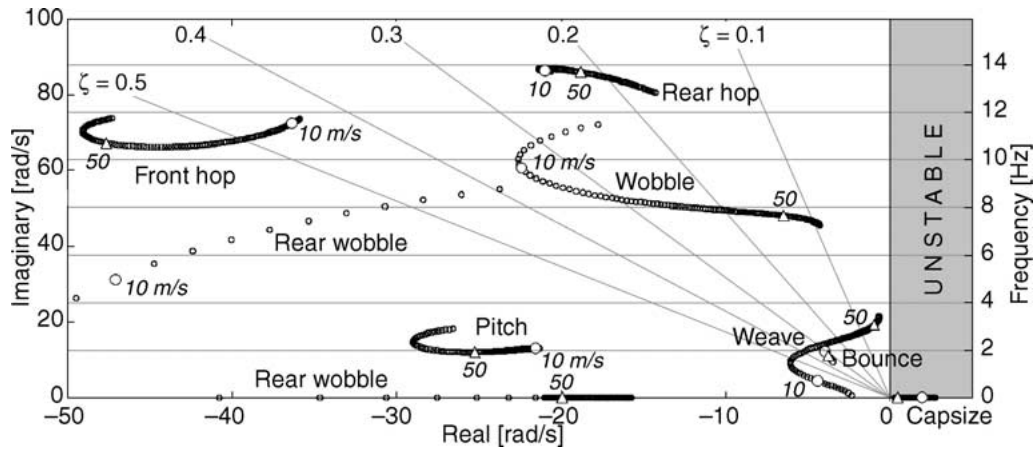


Figure 4. Root locus plot in straight running; speed varies from 5 to 70 m/s.

step of 0.5 m/s). In order to help the reader, the eigenvalues at 10 and 50 m/s are respectively marked with some circular and triangular bigger spots. The graphs are split into two parts to highlight the instability area, which is on the right, in gray. The eigenvalues related to the stable modes fall in the left white area, where some light gray lines show the value of the damping ratios.

Figure 4 shows that in straight running the motorcycle tested has eight significant modes. Their names have been assigned by looking at the modal shape, in accordance with existent published terminology. We can catalogue front hop, rear hop, pitch and bounce as *in-plane* modes, whereas weave, wobble, rear wobble and capsizes are the *out-of-plane* modes. This clear-cut division is possible because of the absence of coupling phenomena. All *in-plane* modes are involved in the definition of the comfort performances of the motorcycle, whereas the remaining modes are of the *out-of-plane* type and deal with motorcycle stability problems. Other modes can be associated to the wheels spinning and vehicle rigid motion, however they are not significant.

The rear hop and the front hop are both characterized by large movements of the unsprung masses (wheels and braking devices) and insignificant displacements of the sprung masses. The frequencies of these modes vary from 10 to 14 Hz and mainly depend on the set-up of the suspensions and on the tires' radial characteristics. Tire and suspension properties also influence the damping ratios, which moderately depend on speed. In particular, the damping of the rear hop decreases as the velocity increases, whereas the damping of the front hop has an opposite evolution. The main reason for this is the variation of the tire vertical load on each wheel due to the aerodynamic effects (load transfer). The vertical load affects the longitudinal slip (modifying the tire rolling radius) and the longitudinal force, on which the dissipation of energy depends. Secondly, it is opportune to observe that the values of the longitudinal forces on the two tires are very different: on the front tire only the rolling resistance acts whereas on the rear one there is the thrust force too. The other *in-plane* modes are characterized by large movements of the sprung mass in the vehicle's symmetry plane. The pitch mainly consists of a rotational movement whereas the bounce mainly consists of vertical hop. Both modes oscillate with a low frequency (from 2 to 3 Hz) because of the great inertia of the sprung mass and the pitch is even more damped than the bounce.

The first *out-of-plane* mode is the capsize, which is always non-vibrational and, for the motorcycle here considered, unstable. Figure 4 shows that it tends to become stable by increasing the speed and we can assert that it is due to the gyroscopic effects of the wheel. The instability of this mode strongly depends on the yaw torque parameters of the front tire, as demonstrated in reference [8]. However, in terms of stability, the most interesting modes remain the weave and the wobble. The weave frequency starts from 0.1 Hz at 5 m/s and increases with the speed until 3.4 Hz at 70 m/s, crossing the frequencies' range of the bounce mode. This fact is fundamental in explaining the modal coupling in the next section. The damping ratio of the weave mode varies from almost 1.00 to 0.03 as the monotonic function of the speed decreases. The wobble mode has a higher frequency which varies from 11.5 Hz at 5 m/s to 7.2 Hz at 70 m/s. Its damping ratio increases in the first part of the speed range (reaching the maximum value of 0.35 at 11 m/s) and then decreases until the value 0.09 at 70 m/s. This final value is very low, even though the motorcycle had a steering damper. The last *out-of-plane* mode shown in Figure 4 is the rear wobble. The shape of this mode is similar to the weave one, but the steering component is more pronounced. The damping ratio is very high at any speed. Its frequency is 8.8 Hz at 5 m/s and quickly decreases as the motorcycle gets faster. At the speed of 12 m/s the frequency becomes null and the mode splits itself into two non-vibrational modes. The first one is visible in the graph (the spots on the real axis), whereas the eigenvalues of the second one are less than -50 and so they are not drawn.

The graphs of Figure 5 show the eigenvalues in steady cornering with lateral accelerations equal, respectively, to 2.5, 5.0 and 7.5 m/s^2 . The lateral inclination of the vehicle is almost proportional to the lateral acceleration (see references [11, 13]) and thus the same graphs represent the vibrational modes with 16° , 31° and 43° of camber angle. The frequency of the wobble depends on both the speed and the lateral acceleration. In particular, as the camber angle increases, the frequency decreases at low speed and increases at high speed. At large camber angles (see Figure 5(c)) the influence of the speed on the frequency becomes very moderate. On the contrary, the velocity always has a strong influence on the stability of the wobble mode. Inside the analyzed speed range, the maximum damping ratio occurs at about 10 m/s. Over this value, stability decreases as speed increases, independently of the camber angle. The lateral acceleration influences stability moving the wobble eigenvalues towards the instability area. As a consequence, at high speeds and large camber angles this mode becomes dangerously unstable.

At very low speeds, the frequency of the weave and bounce modes are clearly different. By increasing the velocity the weave frequency grows whereas the bounce remains almost constant. As a consequence, at 20 m/s both modes oscillate with the same period and this makes possible interactions easy. The modal coupling occurs in Figure 5 where the progression of the weave eigenvalues continues on the branch of the bounce in straight running. Similarly the progression of the bounce eigenvalues continues on the branch that was of the weave in straight running.

The combination of bounce and weave will be further analyzed in the next section using the eigenvectors. It is opportune to observe that the mode names lose their original meaning, because the shapes change substantially. However, the nomenclature will be kept in order to avoid confusion and allow for possible comparison with the existent papers.

The lateral acceleration does not change the frequency of the rear hop, but slightly increases its damping ratio. In fact, when the motorcycle is laterally inclined, the rear wheel hop has a motion component parallel to the ground surface. This component produces a lateral slip that is responsible for the bigger dissipation of energy. On the contrary, the front hop eigenvalues

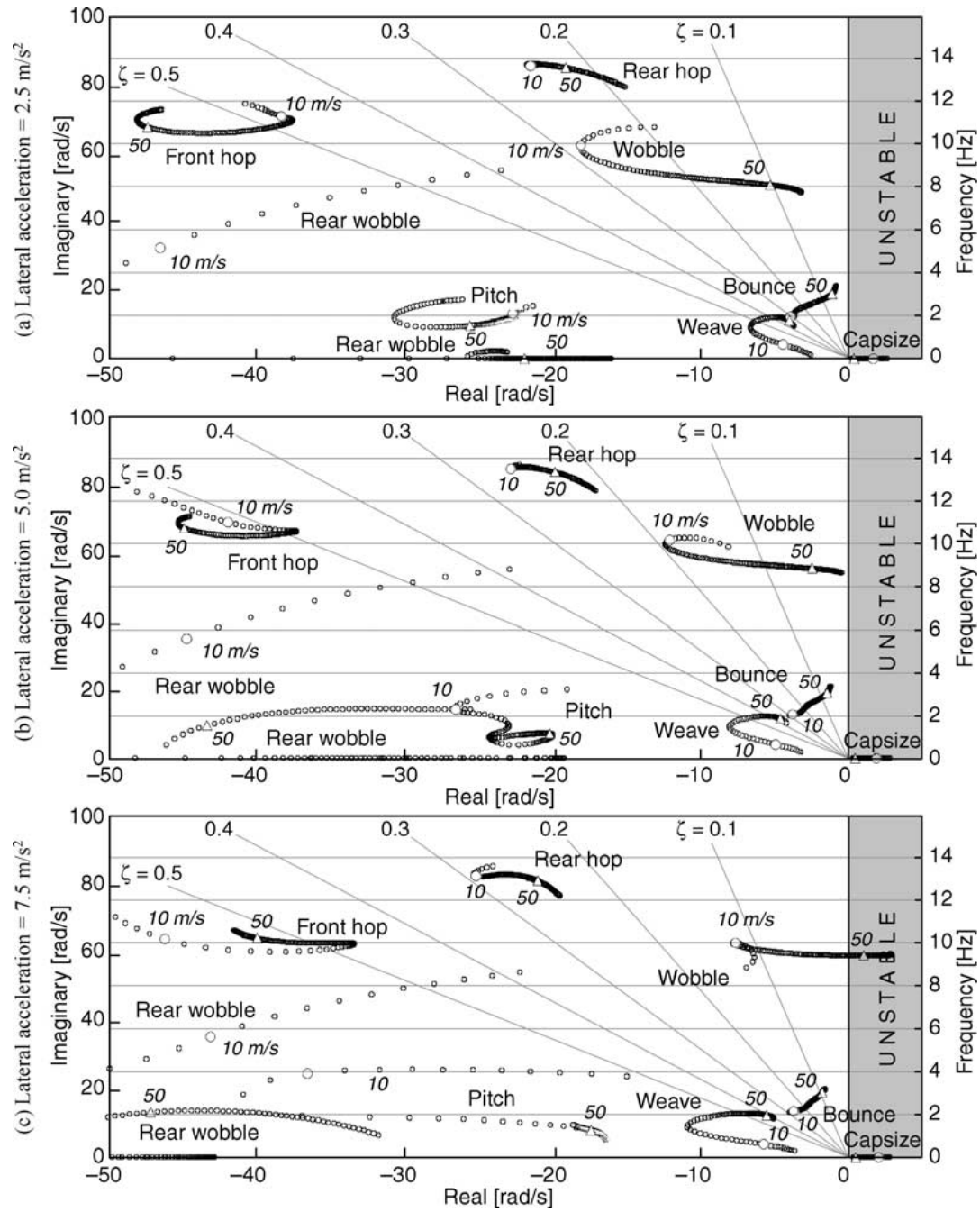


Figure 5. Root locus plot in steady cornering; speed varies from 5 to 70 m/s.

are significantly influenced by the lateral acceleration. Increasing the camber angle (that is going through the Figure 5(a)–(c)) a decrease in the damping ratio of the front hop occurs, but only at low speeds. The frequency stays inside the range 9–13 Hz and its dependence on the speed also varies with the lateral acceleration.

The last *in-plane* mode to be analyzed, is the pitch. The evolution of its eigenvalues strongly depends on the lateral acceleration. At small camber angle (Figure 5(a)), there are

not many differences with the straight running case. On the contrary, when the motorcycle is very inclined, the pitch eigenvalues become more dependent on the speed. This phenomenon represents a further confirmation of the modal coupling. However, the mode remains very stable and its frequency never exceeds 4 Hz.

4.2. EIGENVECTORS

In this section, the eigenvectors of the modes are analyzed. The modal shapes are described using eight components. Five of them are of angular type (the yaw, the camber, the pitch, the steering and the swinging arm angles) whereas the remaining ones are of linear type (lateral displacement, hop displacement and fork travel). It is opportune to specify that the lateral and the hop motion are calculated in the motorcycle reference frame. As a consequence, the hop results vertical and the lateral displacement is horizontal only if the motorcycle is in straight running condition. Since the linear components are not dimensionally homogeneous with the angular ones, they have been transformed into non-dimensional quantities. In particular, the fork deformation has been divided by the wheelbase, obtaining an angle (labeled as fork*) that can be compared with the pitch. The lateral and hop displacements have been divided by the swinging arm length and the resulting angles (labeled as lateral* and hop*) are comparable with the rotation of the swinging arm. As a last step, the eigenvectors are normalized so that the sum of the squares of the components was equal to one.

Each of the figures of this section represents the shape of a single mode and describes how it varies with speed and lateral acceleration. The vector lengths represent the amplitudes of the components, whereas the phase differences are given by the orientation of the vectors. All graphs have the same scale and so the eigenvectors of different modes can be easily compared.

Figure 6 shows the weave shape. First, it is interesting to observe the effects of the speed in straight running motion. The components are the same at low and high speeds (yaw, steer, lateral* and camber), but passing from 10 to 50 m/s, the steering component increases, whereas the lateral* and the camber diminish.

A cornering maneuver causes the coupling between the weave and the bounce. In fact, both at low speeds (first row) and at higher speeds (second row) the hop* and the swinging

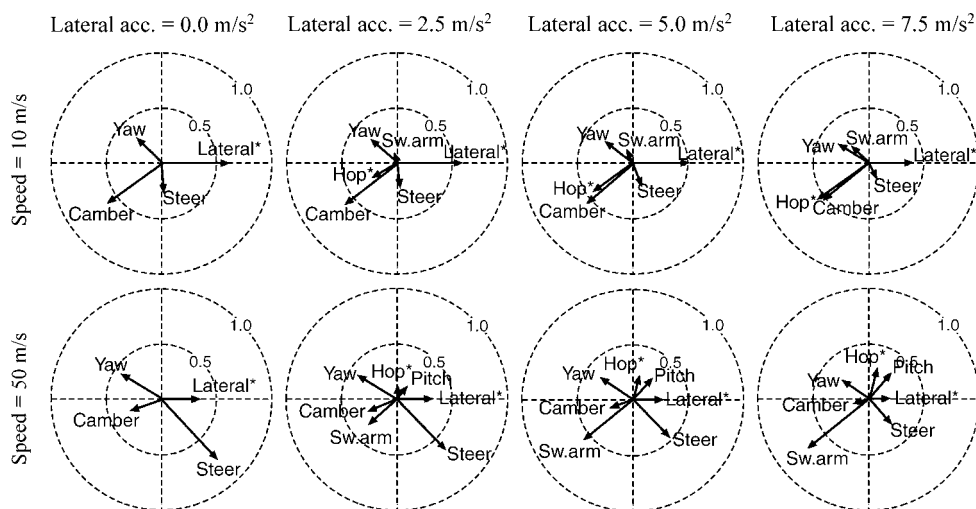


Figure 6. Weave eigenvector.

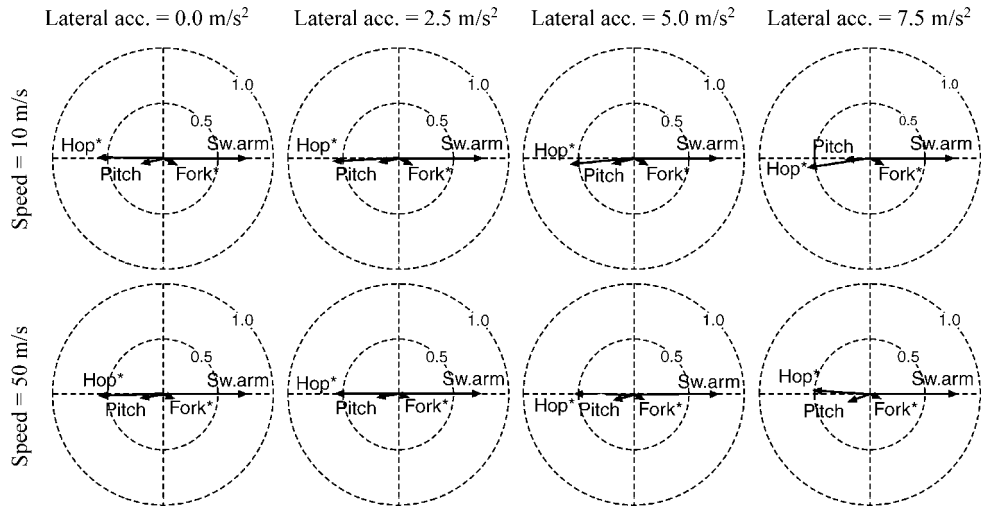


Figure 7. Bounce eigenvector.

arm angle components grow with the lateral acceleration. At 50 m/s the pitch component is also present and has the same evolution. These *in-plane* components are typical of the bounce as is clearly shown in Figure 7. Even if the coupling occurs, the bounce shape does not depend on the speed or on the lateral acceleration. Its main components are the hop* and the swinging arm angle, which are in opposition of phase (when the sprung mass goes up, the swinging arm rotates downward to keep the contact with the ground).

Figure 8 shows the shape of the wobble mode. It consists of a steering oscillation, with an almost imperceptible yaw component (due to the mechanical trail). The short pitch vector that appears when the lateral acceleration is non-zero, confirms the coupling between *in-plane* and *out-of-plane* modes.

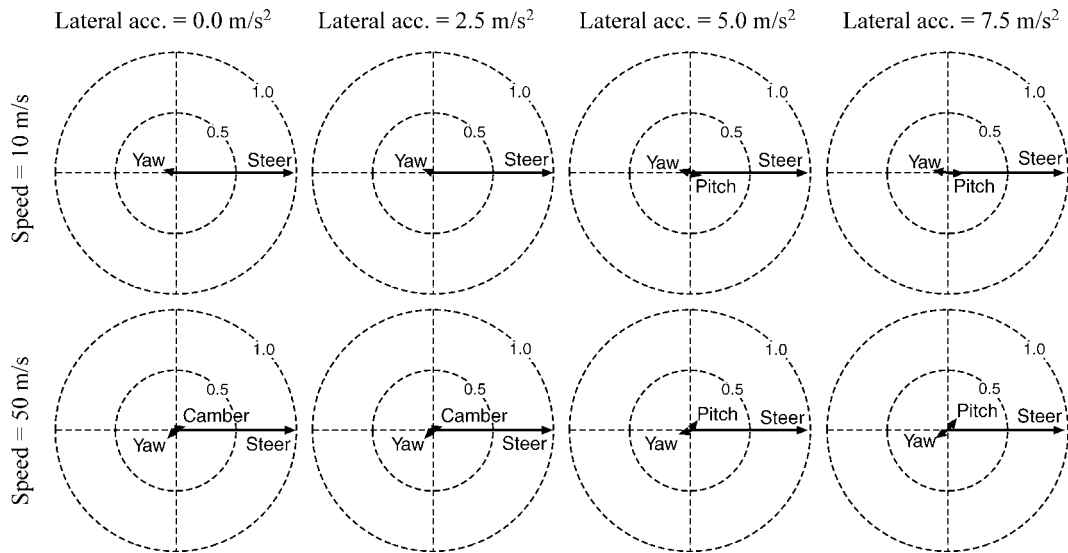


Figure 8. Wobble eigenvector.

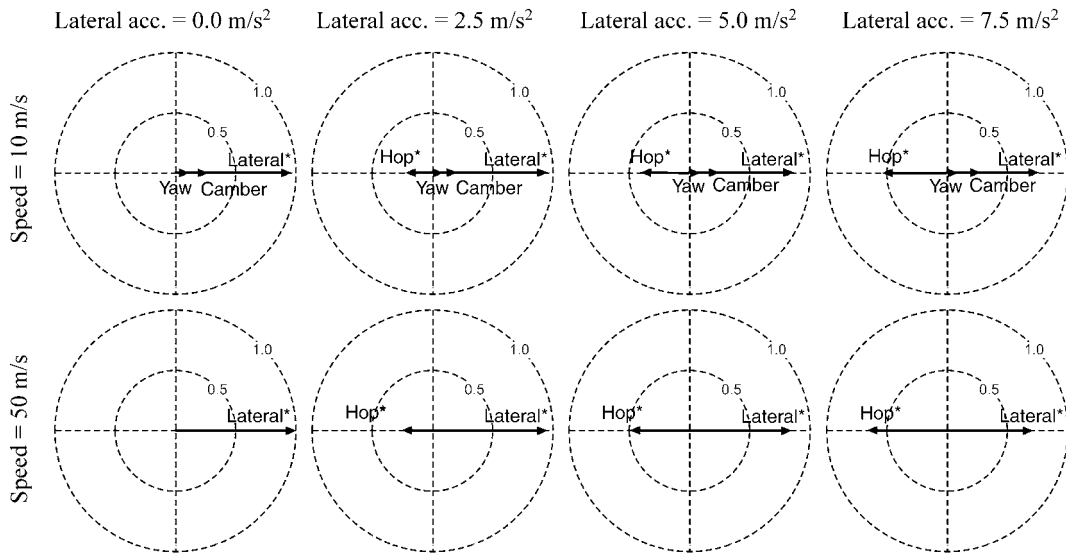


Figure 9. Capsize eigenvector.

Figure 9 represents the capsizing mode, which is the only one of a non-vibrational type. In straight running at slow speed, its components are the lateral* displacement, the yaw and the camber angle. By increasing the speed, yaw and camber components disappear and the capsizing mode becomes a pure horizontal lateral movement. The same thing also happens when the motorcycle is on a curve. It is fundamental to specify that in this case a horizontal displacement generates both a hop* and a lateral* component because of the steady camber angle.

Figure 10 shows the shape of the front hop mode. The presence of a steering angle component in the inclined configurations (second, third and fourth column) confirms that a strong coupling between *in-plane* and *out-of-plane* modes occurs.

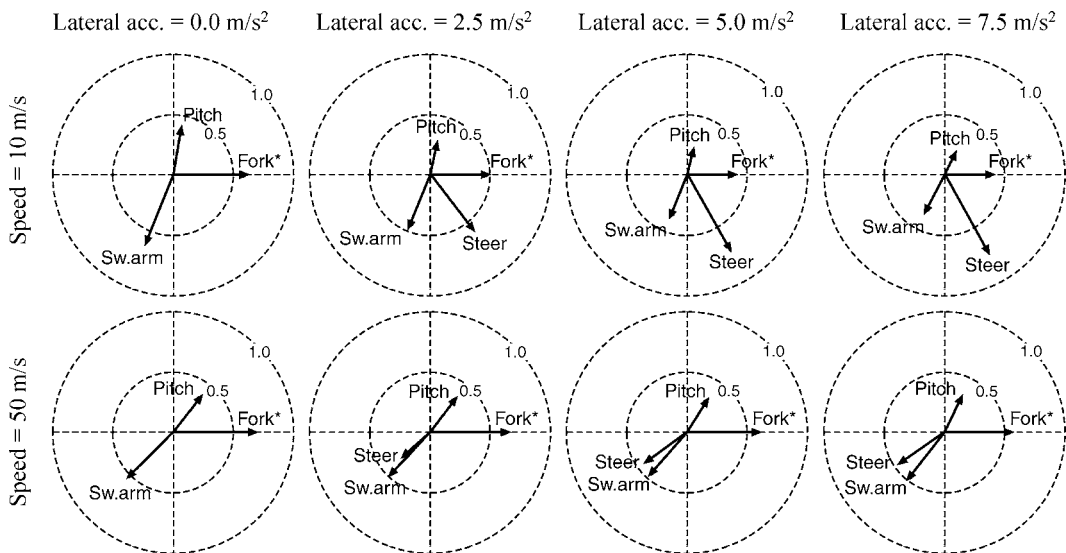


Figure 10. Front hop eigenvector.

The eigenvectors of the rear wobble, pitch and rear hop have not been presented, because they are not particularly interesting. The meaning of the previous graphs was made easier using the eigenvector components for animating the bodies of a 3D graphics model (as shown on the website www.dinamoto.it). The short movies obtained with this method have further highlighted the coupling phenomena.

5. Experimental Tests

In order to validate our results, some experimental tests were done. In the literature, there are many papers on the vibrational modes of the motorcycle, but only a few deal with the experimental aspect of the topic [24, 25]. This shortage of data is due to the practical difficulties in exciting the modes (the main phase of a vibration test). In fact, to obtain a good response signal, the motorcycle should be excited with a very intense impulse. This is commonly reproduced by a hit on the handlebars, but this excitation has some disadvantages. To obtain a free response, the rider should take his hands off the handlebars after the hit and this might be dangerous, especially at high speeds. Moreover, the quantity of energy given by a hit is often too low and the resulting oscillations are imperceptible. Another safer and better procedure is explained in [26]. It consists of running with a small camber angle over a series of bumps. In this case, the front frame is subjected to a succession of impulses, whose frequency depends on the bump distances and on the speed. In the hypothesis of constant speed, it is possible to obtain a frequency sweep from 1 to 12 Hz by fixing the obstacles at decreasing distances. Thus, the motorcycle is excited in the whole range. When the frequency of the external perturbation coincides with one of the free modes resonance occurs.

The experiments were carried out using a sports motorcycle equipped with a steering torque meter, a yaw gyrometer, a camber gyrometer, a lateral accelerometer, a camber inclinometer and a steering angle potentiometer. All signals were sampled at 250 Hz using a digital recorder [19].

The identification of the modes (weave and wobble) and their characteristics [26] consists of two phases. First, it is necessary to identify the stretches of the time history where the resonance is more evident and then these signals have to be processed. Since the system has strong non-linear behavior, the frequency and the damping were extracted using Prony's method [27].

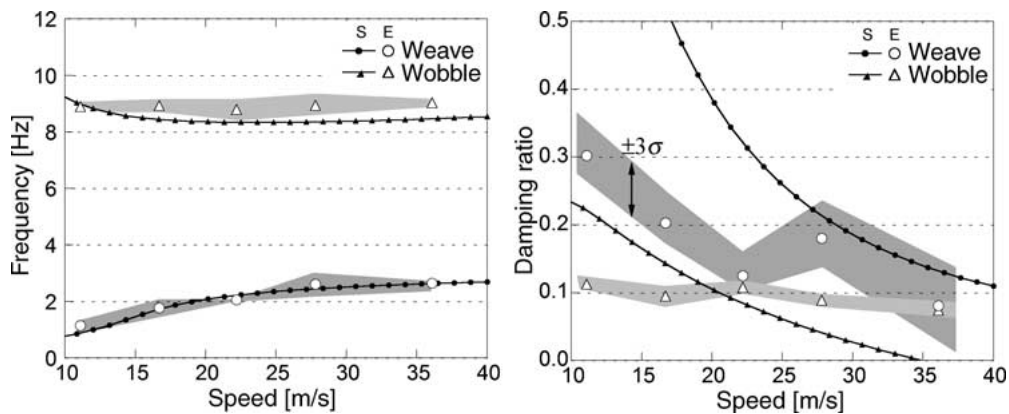


Figure 11. Modes in straight running: comparison between experimental data (E) and simulations (S).

Figure 11 shows the results of the tests and compares them with the simulations. In terms of frequency (left graph), the agreement is very good and this further validates the mathematical model of the motorcycle. On the contrary, the measured damping ratios are rather different from the calculated ones (right graph). The causes could be many. It is opportune to remember that the software makes the modal analysis on a linearized model, whereas the real motorcycle has a strong non-linear behavior. Moreover, many of the parameters of the simulations (such as the tire properties and the suspension properties) were assumed in standard conditions whereas the test conditions were very different. Never the less, these first results are encouraging, and the experimental procedure will be improved upon.

6. Conclusions

The modal analysis of a motorcycle has been presented. The mathematical model used for the numerical analysis was based on a dependent coordinates formulation. An innovative procedure for identifying the equilibrium state was developed. The modes were calculated by linearizing the equations of motion and then dropping out the redundant coordinates.

The results of the eigenvalue problem are given in detail, highlighting the influence of the speed and path curvature on the natural frequency, damping ratio and shape of the modes. In straight running, the *in-plane* and the *out-of-plane* modes are completely uncoupled. The modal coupling occurs when the vehicle is rolled, in particular for the weave and bounce modes, which have similar frequencies. Further modes show weak coupling. The modal shapes are described with the aid of vectorial graphs.

In the experimental section of the paper, a safe and reliable procedure for the test has been described. The measured parameters of the weave and the wobble have been compared with the numerical results, finding a good agreement.

Acknowledgements

This research was partially supported by funds from the Italian Ministry for Universities and for Scientific and Technological Research (MURST 40% funds). The authors also thank M. Rigamonti for his collaboration in the processing of the experimental data.

References

1. Sharp, R.S., 'The stability and control of motorcycles', *J. Mech. Eng. Sci.* **13** (1971).
2. Sharp, R. S., 'The influence of frame flexibility on the lateral stability of motorcycles', *J. Mech. Eng. Sci.* **16** (1974).
3. Kane, T.R., *The Effect of Frame Flexibility on High Speed Weave of Motorcycles*, SAE Paper **780306**, 1978.
4. Verma, M.K., Scott, R.A. and Segel, L., 'Effect of frame compliance on the lateral dynamics of motorcycles', *Vehicle Syst. Dyn.* **9** (1980).
5. Cossalter, V., Doria, A. and Mitolo, L., *Inertial and Modal Properties of Racing Motorcycles*, SAE Paper 2002-01-**3347**, 2002.
6. Sharp, R.S. and Alstead, C.J., 'The influence of structural flexibilities on the straight-running stability of motorcycles', *Vehicle Syst. Dyn.* **9** (1980).
7. Spierings, P.T.J., 'The effect of lateral front fork flexibility on the vibrational modes of straight-running single-track vehicles', *Vehicle Syst. Dyn.* **10** (1981).
8. Cossalter, V., Lot, R. and Maggio, F., *The Influence of Tire Properties on the Stability of a Motorcycle in Straight Running and Curves*, SAE Paper 2002-01-**1572**, 2002.

9. Takahashi, T., Yamada, T. and Nakamura, T., *Experimental and Theoretical Study of the Influence of Tires Properties on Straight-running Weave Response*, SAE Paper **840248**, 1984.
10. Katayama, T. and Nishimi, T., 'Energy flow method for the study of motorcycle wobble mode', *Vehicle Syst. Dyn.* **19** (1990).
11. Koenen, C. and Pacejka, H.B., 'Vibrational modes of motorcycles in curve', in: *Proc. Int. Motorcycle Safety Conf.*, Washington D.C., 1980.
12. Koenen, C. and Pacejka, H.B., 'Influence of frame elasticity, simple rider body dynamics and tyre moments on free vibrations of motorcycles in curves', in: *Proc. IAVSD Symposium*, 1982.
13. Maggio, F., *Modi di Vibrare della Motocicletta: Accoppiamenti tra Modi Laterali e Verticali*, Degree Thesis University of Padova, 2001 (in Italian).
14. Sharp, R.S., 'Stability, control and steering responses of motorcycles', *Vehicle Syst. Dyn.* **35** (2001).
15. Cossalter, V. and Lot, R., 'A motorcycle multi-body model for real time simulations based on the natural coordinates approach', *Vehicle Syst. Dyn.* **37** (2002) 423–447.
16. Da Lio, M. and Lot, R., 'Analisi modale di sistemi multi-body descritti in coordinate naturali', in: *XIV Congresso AIMETA*, Como, 1999 (in Italian).
17. Bajo, E. and de Jalon, J.C., *Kinematic and Dynamic Simulation of Multibody Systems*, Springer-Verlag, New York, 1994.
18. Sush, H. and Radcliffe, C.W., *Kinematics and Mechanism Design*, Chapter 3, John Wiley & Sons, New York, 1978.
19. Bortoluzzi, D., Doria, A., Lot, R. and Fabbri, L., 'Experimental investigation and simulation of motorcycle turning performance', in: *Proc. 3rd Int. Motorrad-Konferenzen*, Monaco, 2000.
20. Cossalter, V., 'Motorcycle dynamics', *RDI* (2002) (in press).
21. Pacejka, H.B. and Bakker, E., 'The magic formula tyre model', *Vehicle Syst. Dyn.* **21** (Supplement) (1991).
22. Sakay, H., 'Study on cornering properties of tire and vehicle', *Tire Sci. Tech.* **18** (1990).
23. Pacejka, H.B. and Sharp, R.S., 'Shear force development by pneumatic tyres in steady state conditions: a review of modelling aspects', *Vehicle Syst. Dyn.* **20** (1991).
24. Verma, M.K., *Theoretical and Experimental Investigations of Motorcycle Dynamics*, Ph.D. Dissertation, The University of Michigan, 1978.
25. Bayer, V.B., *Das Pendeln und Flattern von Krafträdern*, Institut für Zweiradsicherheit e. V. Bochum, 1986.
26. Rigamonti, M., *Dinamica Laterale della Motocicletta: Identificazione Sperimentale dei Modi di Vibrare Weave e Wobble*, Degree Thesis, Politecnico di Milano, 2002 (in Italian).
27. Marple, S.L., *Digital Spectral Analysis with Applications*, Prentice-Hall, 1987.
28. Lot, R., 'A motorcycle tire model for dynamic simulations: theoretical and experimental aspects', in: *Proc. 3rd Int. AIMETA Tribology Conf.*, 18–20 September 2002, Vietri sul Mare, Salerno, Italy.